Dark Matter: Direct (Mineral) Detection

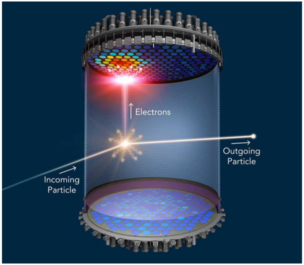

Figure: LZ Collaboration

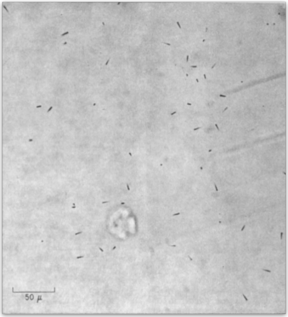

Figure: Price+Walker '63

Jožef Stefan Institute
Ljubljana, Slovenia

SMASH
machine learning for science and humanities postdoctoral program

Co-funded by the European Union

This project has received funding from the European Union's Horizon Europe research and innovation programme under the Marie Skłodowska-Curie grant agreement No. 101081355.

Outline

1. Dark matter recoiling off nuclei
2. Backgrounds
    - Astrophysical neutrinos
    - Cosmogenic muons
    - Radiogenic
3. Mineral detectors for dark matter

What do we (not) know about dark matter?

What we (typically) assume

- No E&M interactions
- Must be cold and stable
- Not in the Standard Model

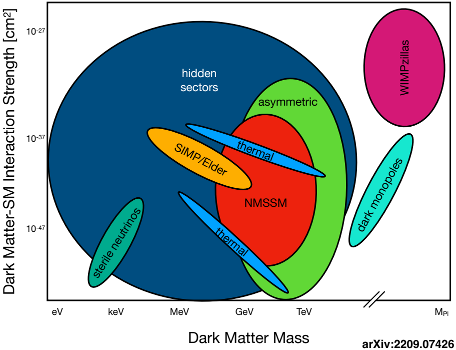

arXiv:2209.07426

SLAC National Accelerator Laboratory

Limits on dark matter interactions with nucleons

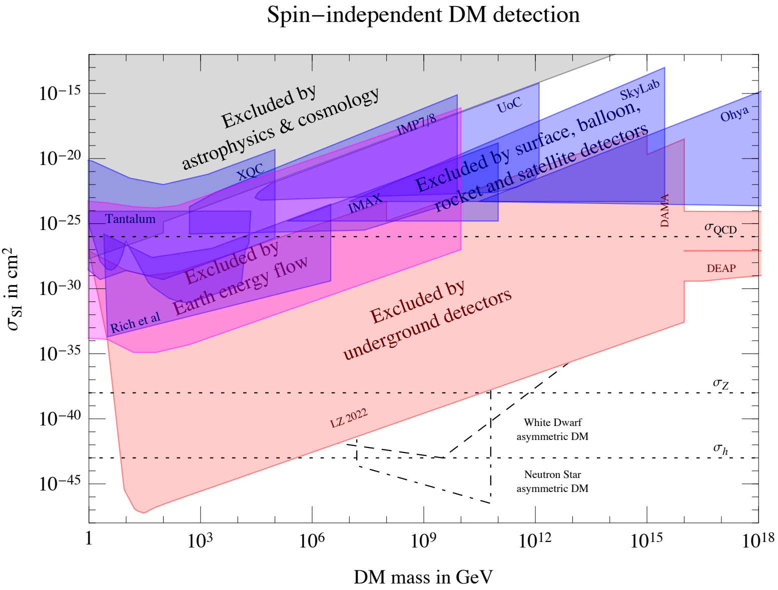

Limits from current direct detection experiments

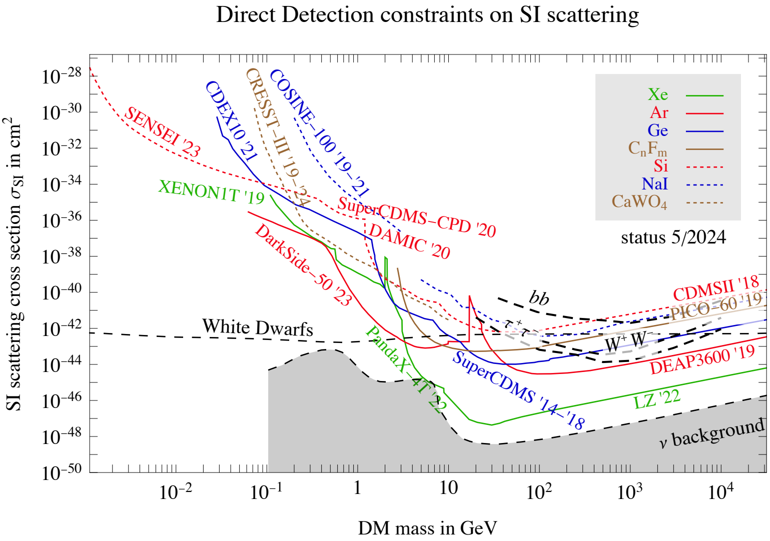

Figure: 2406.01705

Projected sensitivity of future direct detection experiments

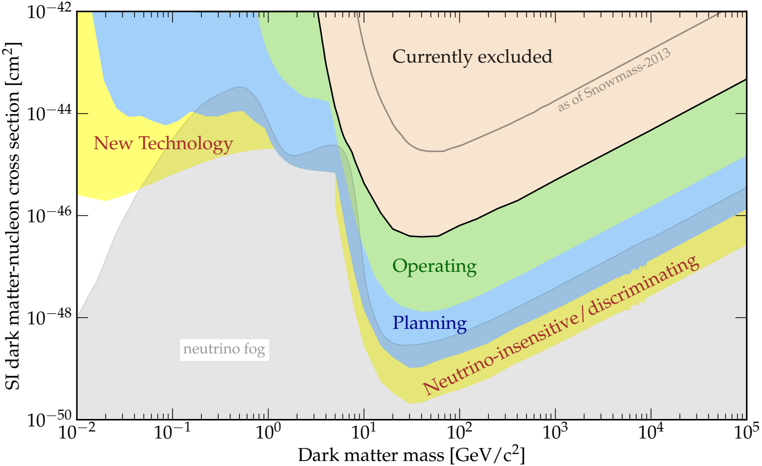

Figure: 2209.07426

Characteristic dark matter interactions with nucleons

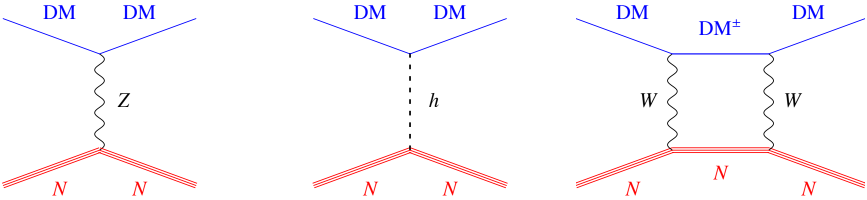

tree, vector

$$\sigma_{\rm SI} \approx \frac{\alpha^2\, m_N^2}{M_Z^4}$$

tree, scalar

$$\sigma_{\rm SI} \approx \frac{\alpha^2\, m_N^4}{M_h^6}$$

loop

$$\sigma_{\rm SI} \approx \frac{\alpha^4\, m_N^4}{M_W^6}$$

Figure: 2406.01705

Scattering cross sections ⇒ scattering rates

$$\frac{d^2\sigma}{dq^2 d\Omega_q} = \frac{d\sigma}{dq^2}\frac{1}{2\pi}\delta\left(\cos\theta - \frac{q}{2\mu_{XT} v}\right) \simeq \frac{\sigma_0 F(q)^2}{8\pi\mu_{XT}^2 v}\delta\left(v\cos\theta - \frac{q}{2\mu_{XT}}\right)$$

$$\frac{d^2R}{dE_R d\Omega_q} = 2M_T\frac{N_T}{M_T N_T}\int\frac{d^2\sigma}{dq^2 d\Omega_q} n_X\, v\, f(\boldsymbol{v}) d^3v \simeq \frac{\sigma_0 F(q)^2}{4\pi\mu_{XT}} n_X \hat{f}(v_q, \hat{\boldsymbol{q}})$$

Differential cross section

- δ-function imposes kinematics
- σ_0 is velocity and momentum independent cross section for scattering off pointlike nucleus

$$F(q) \simeq \frac{9\,[\sin(qR) - qR\cos(qR)]^2}{(qR)^6}$$

Differential scattering rate

- Rate per unit time per unit detector mass for all nuclei
- Convolute cross section with astrophysical WIMP flux

$$\sigma_0^{SI} = \frac{4}{\pi}\mu_{XT}^2\left[Zf_s^p + (A-Z)f_s^n\right]^2$$

Dark matter density in the galaxy

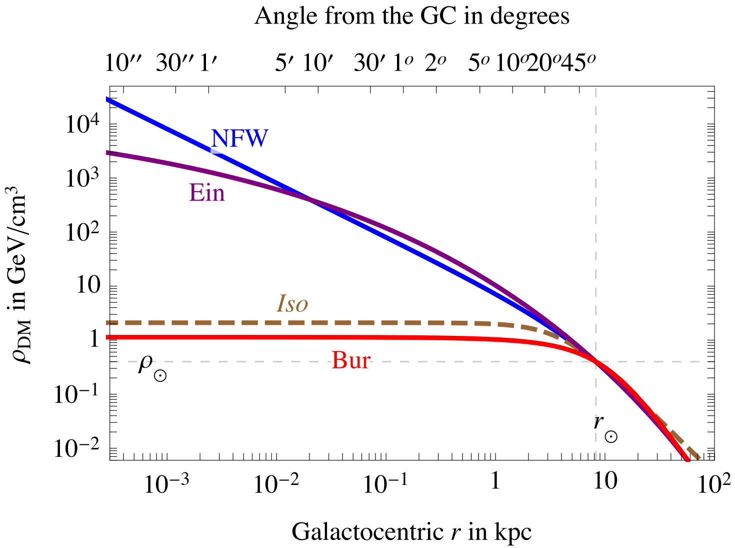

Figure: 2406.01705

Velocity distribution in the Standard Halo Model (SHM)

Integrate Radon transform

$$\int \hat{f}(v_q, \hat{\boldsymbol{q}})d\Omega_q = 2\pi\eta(v_q)$$

Mean inverse speed

$$\eta(v_q) = \int_{v>v_q} \frac{f(\boldsymbol{v})}{v} d^3v$$

Maxwellian in halo frame

$$\tilde{f}(\boldsymbol{v}) \sim \left(\frac{3}{2\pi\sigma_v^2}\right)^{3/2} e^{-3v^2/2\sigma_v^2}$$

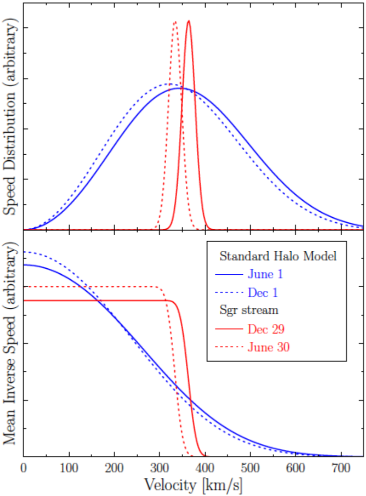

Figure: 1209.3339

Spin- and velocity-independent WIMP-nucleus scattering

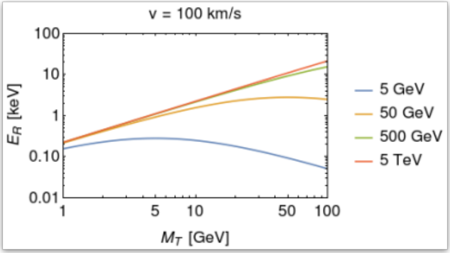

Scattering kinematics ⇒ event rate

- Account for finite size of nucleus
- Convolute with WIMP flux
- Write cross section in terms of WIMP-nucleon interaction

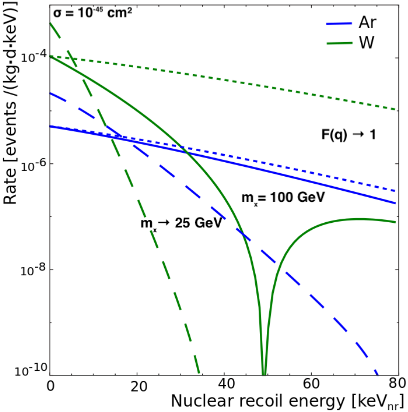

Figure: 1509.08767

$$\frac{dR}{dE_R} = \frac{n_X}{2}\frac{\sigma^{SI}_{Xp}}{\mu^2_{Xp}} A^2 F(q)^2 \eta(v_q)$$

Example bracketing impact of astrophysical uncertainties

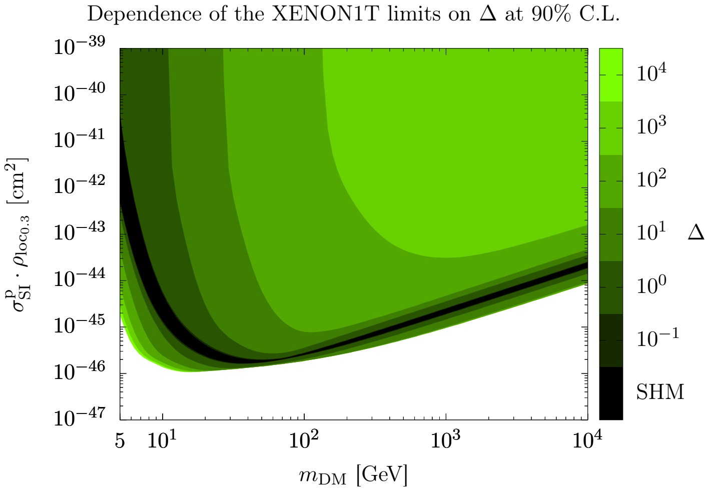

Figure: 1806.08714, variations of σ_v and $v_{\rm esc}$ in SHM and variations away from MB in SHM $\Delta \leq |f(\boldsymbol{v}) - f_{MB}(\boldsymbol{v})|/f_{MB}(\boldsymbol{v})$ for $f(\boldsymbol{v})$ composed of DM streams

Conventional direct detection experiments

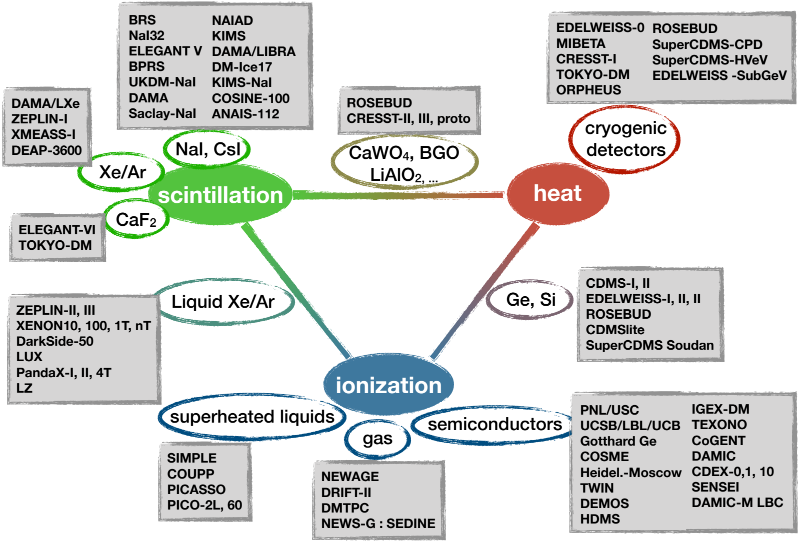

DAMA/LXe
ZEPLIN-I
XMEASS-I
DEAP-3600

BRS
NaI32
ELEGANT V
BPRS
UKDM-NaI
DAMA
Saclay-NaI
NAIAD
KIMS
DAMA/LIBRA
DM-Ice17
KIMS-NaI
COSINE-100
ANAIS-112

ROSEBUD
CRESST-II, III, proto

EDELWEISS-0
MIBETA
CRESST-I
TOKYO-DM
ORPHEUS
ROSEBUD
SuperCDMS-CPD
SuperCDMS-HVeV
EDELWEISS -SubGeV

ELEGANT-VI
TOKYO-DM

ZEPLIN-II, III
XENON10, 100, 1T, nT
DarkSide-50
LUX
PandaX-I, II, 4T
LZ

CDMS-I, II
EDELWEISS-I, II, II
ROSEBUD
CDMSlite
SuperCDMS Soudan

SIMPLE
COUPP
PICASSO
PICO-2L, 60

NEWAGE
DRIFT-II
DMTPC
NEWS-G : SEDINE

PNL/USC
UCSB/LBL/UCB
Gotthard Ge
COSME
Heidel.-Moscow
TWIN
DEMOS
HDMS
IGEX-DM
TEXONO
CoGENT
DAMIC
CDEX-0,1, 10
SENSEI
DAMIC-M LBC

Figure: 2406.01705

Neutrinos come from a variety of sources

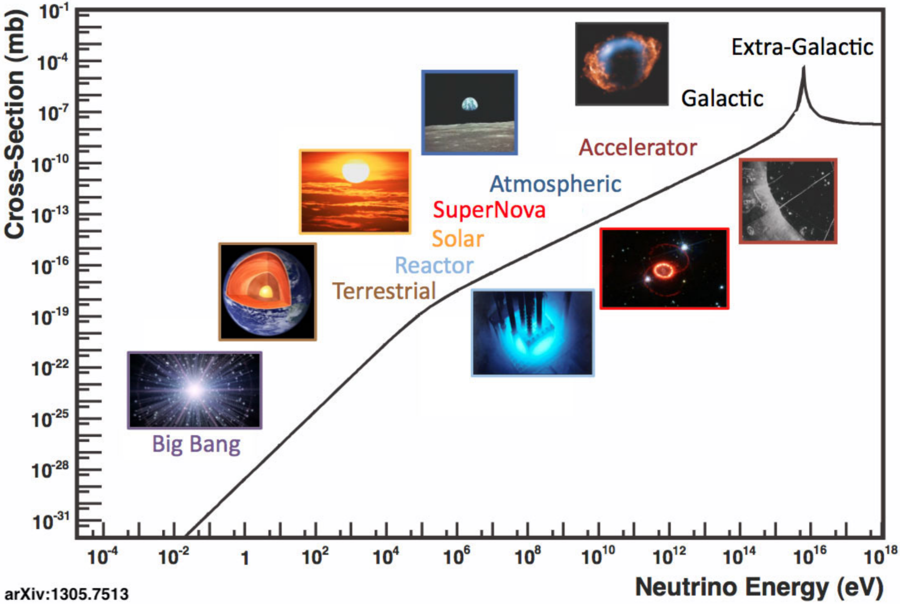

arXiv:1305.7513

Nuclear recoil spectrum depends on neutrino energy

$$\frac{dR}{dE_R} = \frac{1}{m_T} \int dE_\nu \, \frac{d\sigma}{dE_R} \frac{d\phi}{dE_\nu}$$

- Quasi-elastic for $E_\nu \gtrsim 100\,\mathrm{MeV}$
- Resonant π production at $E_\nu \sim \mathrm{GeV}$
- Deep inelastic for $E_\nu \gtrsim 10\,\mathrm{GeV}$

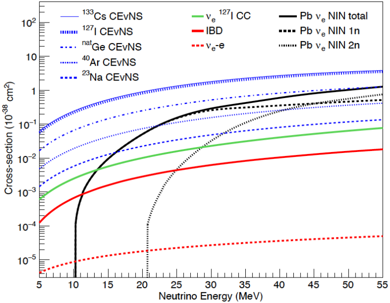

Figure: COHERENT, 1803.09183

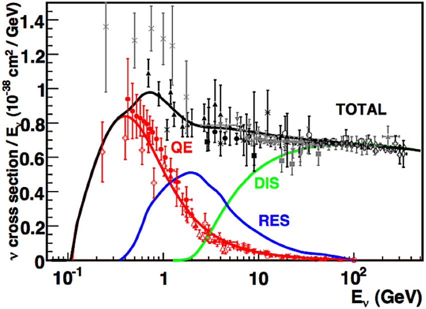

Figure: Inclusive CC $\sigma_{\nu N}$, 1305.7513

Atmospheric μ's and ν's originating from CR interactions

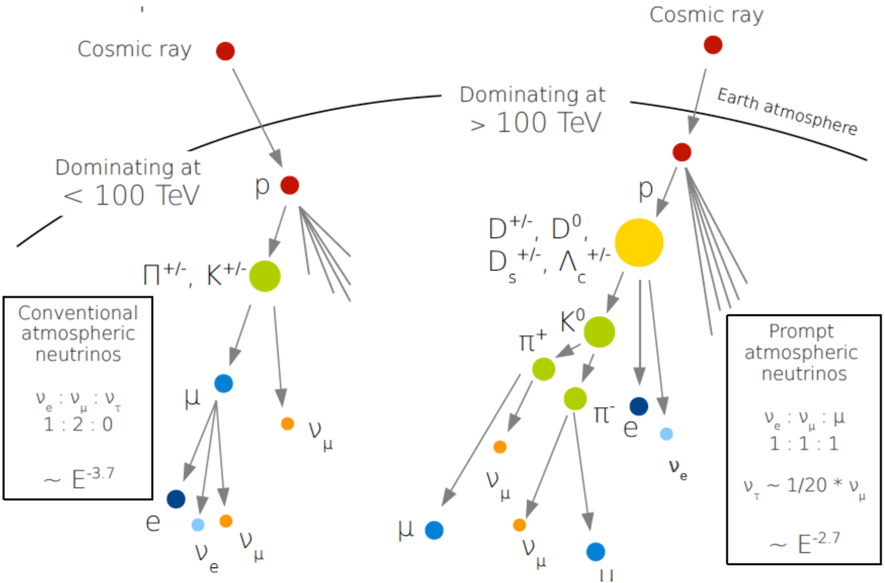

Conventional atmospheric neutrinos

$\nu_e : \nu_\mu : \nu_\tau$
1 : 2 : 0

$\sim E^{-3.7}$

Prompt atmospheric neutrinos

$\nu_e : \nu_\mu : \mu$
1 : 1 : 1

$\nu_\tau \sim 1/20 * \nu_\mu$

$\sim E^{-2.7}$

Courtesy: Anne Schukraft

Atmospheric μ and ν_μ fluxes

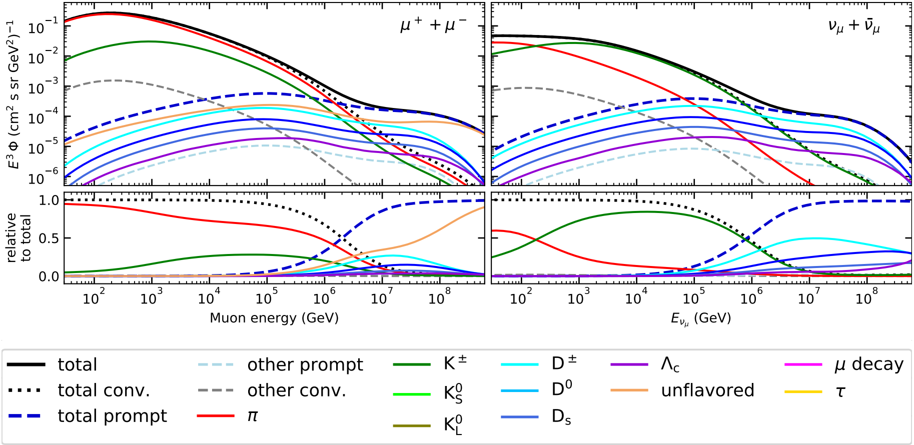

Figure: 1806.04140

Atmospheric ν energy depends on CR energy and angle

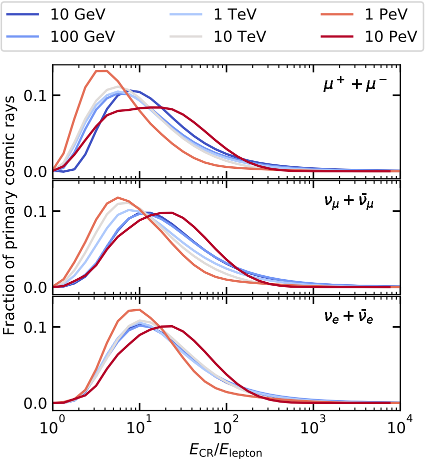

Figure: E_{CR} to leptons, 1806.04140

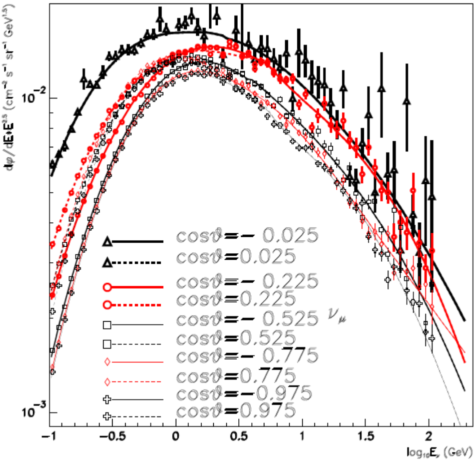

Figure: FLUKA simulation of ν_μ flux at SuperK for solar max, hep-ph/0207035

Core collapse supernova ν's

Only ~ 2 SN 1987A events/century

- Measure galactic CC SN rate
- Traces star formation history

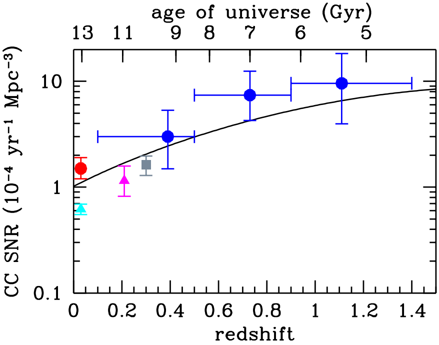

Figure: 1403.0007

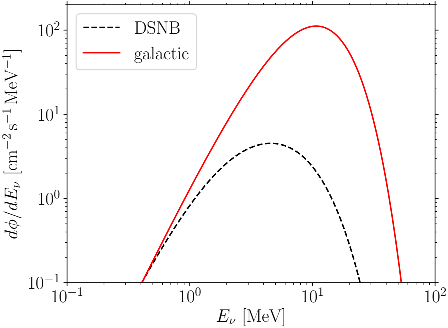

Figure: 1906.05800

Solar ν's produced in fusion chains from H to He

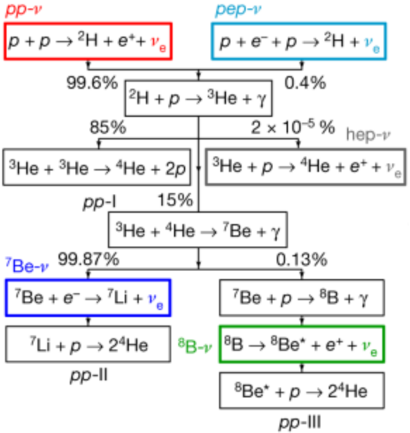

pp-ν

$p + p \to {}^2H + e^+ + \nu_e$

pep-ν

$p + e^- + p \to {}^2H + \nu_e$

99.6%

0.4%

${}^2H + p \to {}^3He + \gamma$

85%

2×10^{-5} %

hep-ν

${}^3He + {}^3He \to {}^4He + 2p$

${}^3He + p \to {}^4He + e^+ + \nu_e$

pp-I

15%

${}^3He + {}^4He \to {}^7Be + \gamma$

^{7}Be-ν

99.87%

0.13%

${}^7Be + e^- \to {}^7Li + \nu_e$

${}^7Be + p \to {}^8B + \gamma$

${}^7Li + p \to 2{}^4He$

^{8}B-ν

${}^8B \to {}^8Be^* + e^+ + \nu_e$

pp-II

${}^8Be^* + p \to 2{}^4He$

pp-III

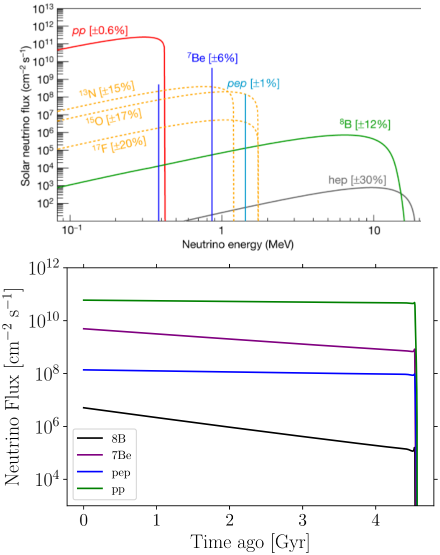

Figure: Today's flux at Borexino (Nature, 2018) and time dependence of GS metallicity model, 2102.01755

Cosmogenic muons induce fast neutrons underground

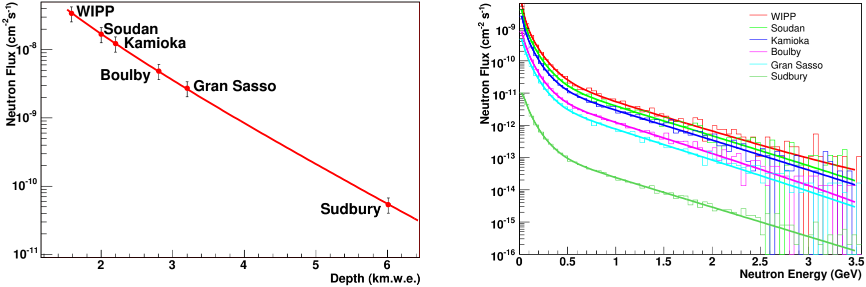

Figure: astro-ph/0512125

Cosmogenic backgrounds suppressed in deep boreholes

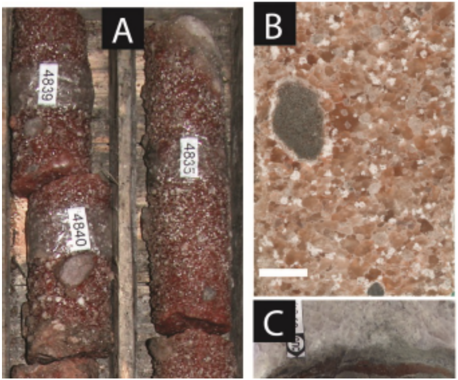

Figure: $\sim$ 2Gyr old Halite cores from $\sim$ 3km, as discussed in Blättler+ '18

Depth	Neutron Flux
2 km	$10^6/\mathrm{cm}^2/\mathrm{Gyr}$
5 km	$10^2/\mathrm{cm}^2/\mathrm{Gyr}$
6 km	$10/\mathrm{cm}^2/\mathrm{Gyr}$
50 m	$70/\mathrm{cm}^2/\mathrm{yr}$
100 m	$30/\mathrm{cm}^2/\mathrm{yr}$
500 m	$2/\mathrm{cm}^2/\mathrm{yr}$

Need minerals with low ^{238}U

- Marine evaporites with $C^{238} \gtrsim 0.01$ ppb
- Ultra-basic rocks from mantle, $C^{238} \gtrsim 0.1$ ppb

Radiogenic backgrounds from ^{238}U contamination

$$^{238}\mathrm{U} \xrightarrow{\alpha} {}^{234}\mathrm{Th} \xrightarrow{\beta^-} {}^{234\mathrm{m}}\mathrm{Pa} \xrightarrow{\beta^-} {}^{234}\mathrm{U} \xrightarrow{\alpha} {}^{230}\mathrm{Th} \xrightarrow{\alpha} {}^{226}\mathrm{Ra} \xrightarrow{\alpha} {}^{222}\mathrm{Rn} \xrightarrow{\alpha} \ldots \longrightarrow {}^{206}\mathrm{Pb}$$

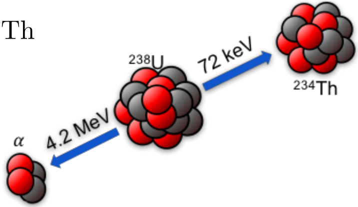

Nucleus	Decay mode	$T_{1/2}$
^{238}U	α SF	4.468×10^9 yr 8.2×10^{15} yr
^{234}Th	β^-	24.10 d
$^{234\mathrm{m}}$Pa	β^- (99.84 %) IT (0.16 %)	1.159 min
^{234}Pa	β^-	6.70 d
^{234}U	α	2.455×10^5 yr

"1α" events difficult to reject without additional decays

- Reject $\sim 10\,\mu$m α tracks
- Without α tracks, filter out monoenergetic ^{234}Th

Fast neutrons from SF and (α, n) interactions

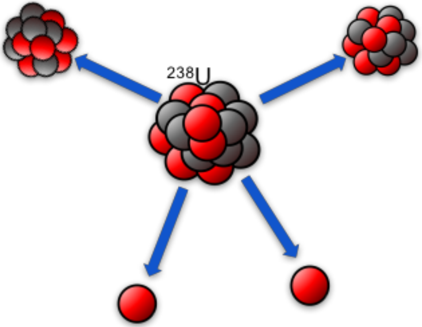

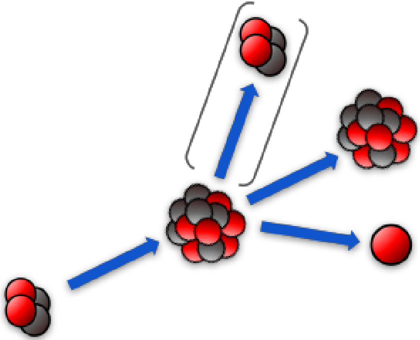

SF yields ∼ 2 neutrons with ∼MeV

Each neutron will scatter elastically 10-1000 times before moderating

(α, n) rate low, many decay α's

Heavy targets better for (α, n) and bad for neutron moderation, need H

Quick aside on data analysis and α-recoil background

- 15 nm resolution of 100 g sample
  $\Rightarrow 10^{19}$ mostly empty voxels
- 1 Gyr old with $C^{238} = 0.01$ ppb
  $\Rightarrow 10^{13}$ voxels for α-recoil tracks

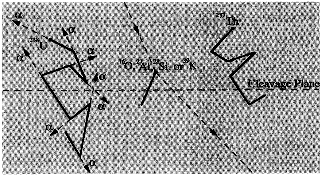

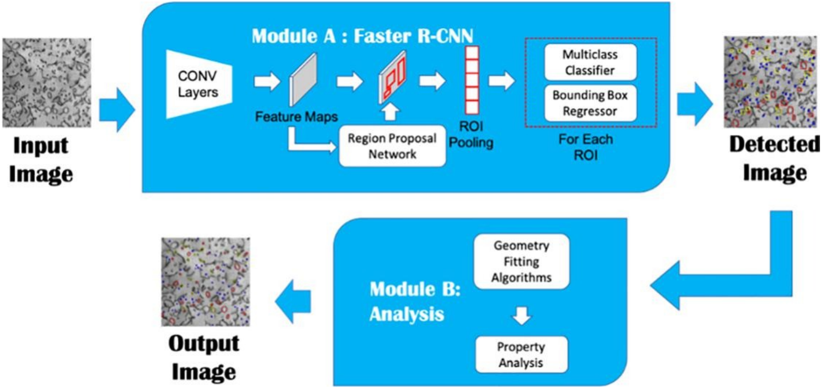

Outline

1. Dark matter recoiling off nuclei

2. Backgrounds
   - Astrophysical neutrinos
   - Cosmogenic muons
   - Radiogenic

3. Mineral detectors for dark matter

Putting together all of the signals and backgrounds

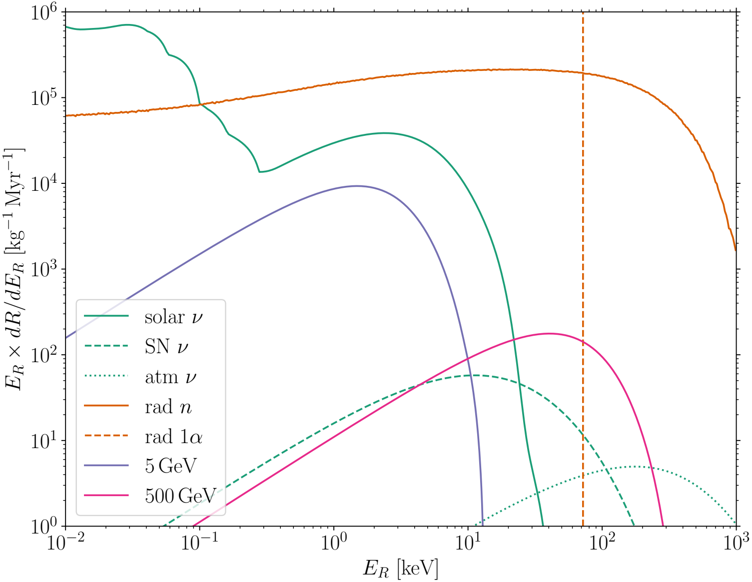

Mineral detectors used to constrain WIMPs before

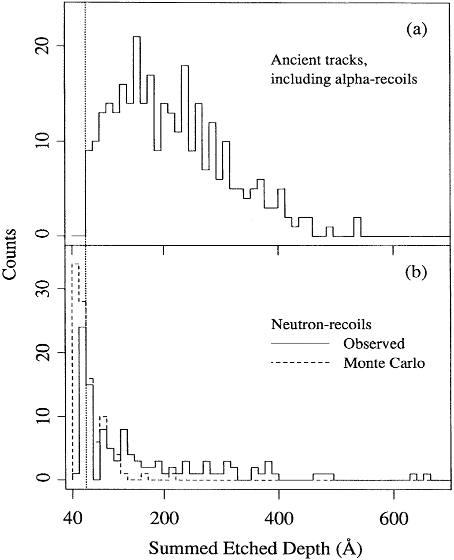

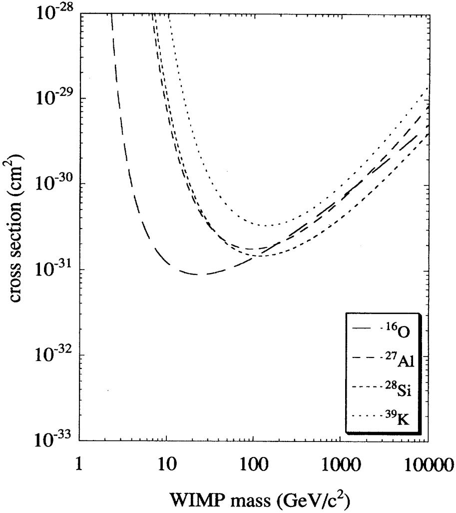

Figure: Snowden-Ifft et al. (1995)

New techniques allow for much larger readout capacity

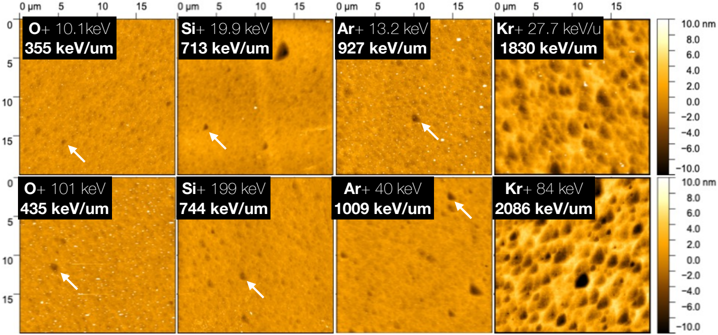

Irradiation dose is 80 ions per field of view (20umx20um).

proxy	DM scattering	alpha recoils
pit formation efficiency	several to 10 %	~ 100%

Color centers can be used to probe low mass dark matter

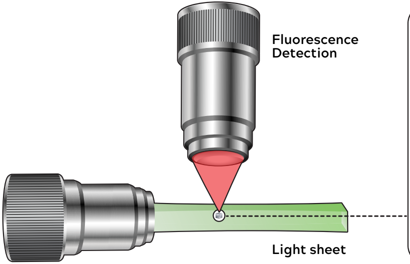

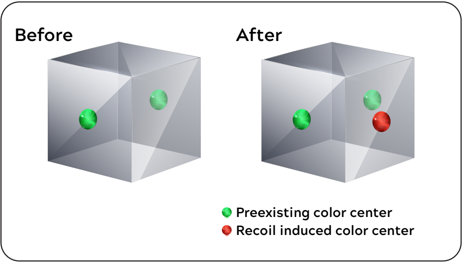

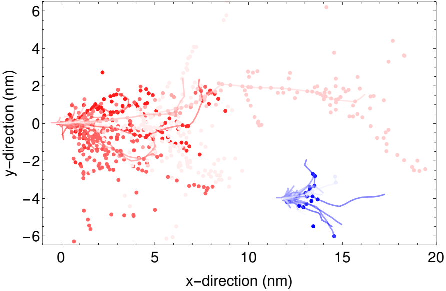

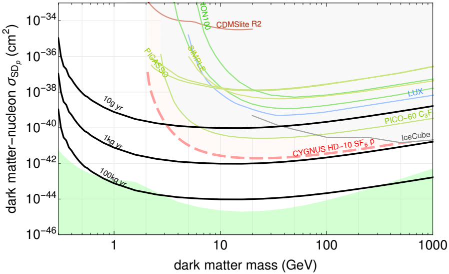

Mineral detectors look for damage from recoiling nuclei

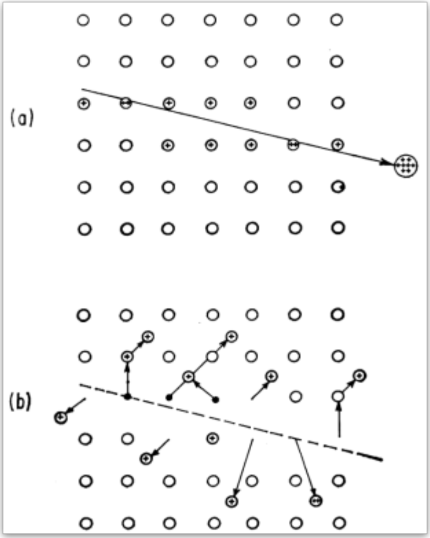

Track length from stopping power

$$x_T(E_R) = \int_0^{E_R} dE \left| \frac{dE}{dx_T}(E) \right|^{-1}$$

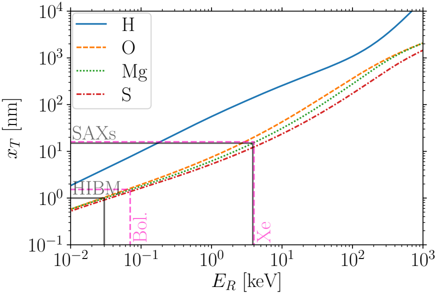

Track length spectra for various mineral targets

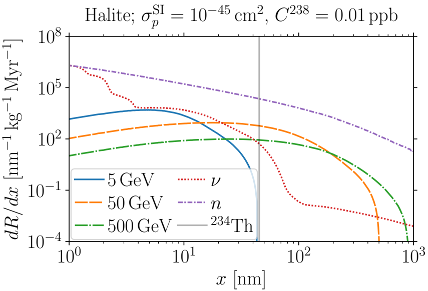

Halite; $\sigma_p^{\mathrm{SI}} = 10^{-45}\,\mathrm{cm}^2$, $C^{238} = 0.01\,\mathrm{ppb}$

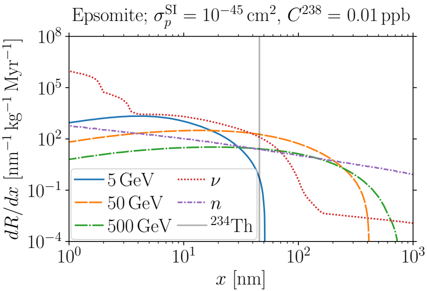

Epsomite; $\sigma_p^{\mathrm{SI}} = 10^{-45}\,\mathrm{cm}^2$, $C^{238} = 0.01\,\mathrm{ppb}$

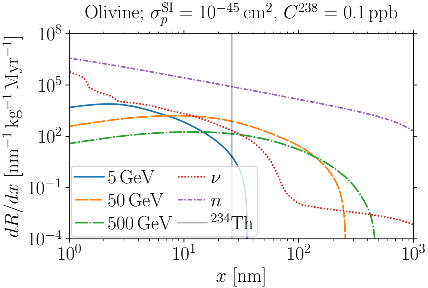

Olivine; $\sigma_p^{\mathrm{SI}} = 10^{-45}\,\mathrm{cm}^2$, $C^{238} = 0.1\,\mathrm{ppb}$

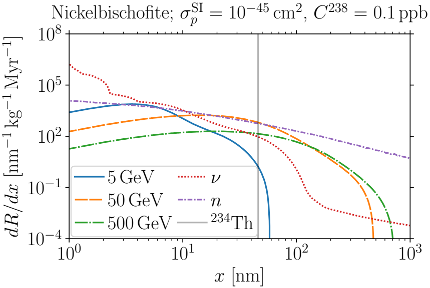

Nickelbischofite; $\sigma_p^{\mathrm{SI}} = 10^{-45}\,\mathrm{cm}^2$, $C^{238} = 0.1\,\mathrm{ppb}$

Track length spectra after smearing by readout resolution

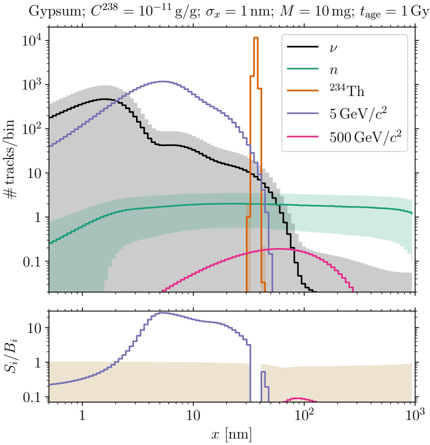

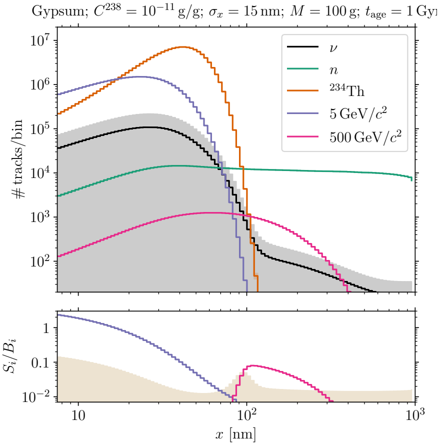

Sensitivity for different targets

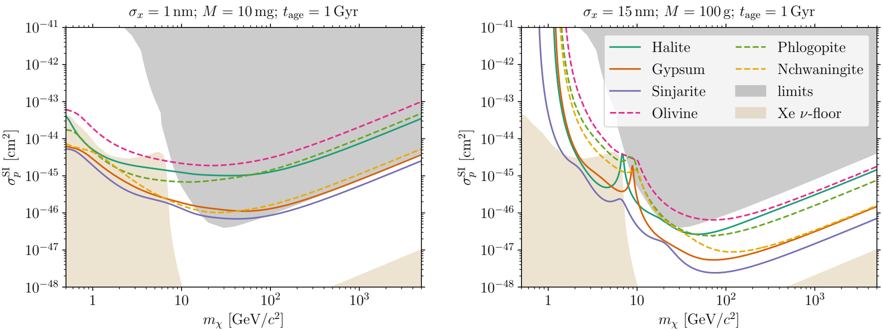

Halite	NaCl	$C^{238} = 10^{-11}$ g/g
Gypsum	$Ca(SO_4){\cdot}2(H_2O)$	$C^{238} = 10^{-11}$ g/g
Sinjarite	$CaCl_2{\cdot}2(H_2O)$	$C^{238} = 10^{-11}$ g/g
Olivine	$Mg_{1.6}Fe^{2+}_{0.4}(SiO_4)$	$C^{238} = 10^{-10}$ g/g
Phlogopite	$KMg_3AlSi_3O_{10}F(OH)$	$C^{238} = 10^{-10}$ g/g
Nchwaningite	$Mn^{2+}_2SiO_3(OH)_2{\cdot}(H_2O)$	$C^{238} = 10^{-10}$ g/g

Effects of background shape systematics

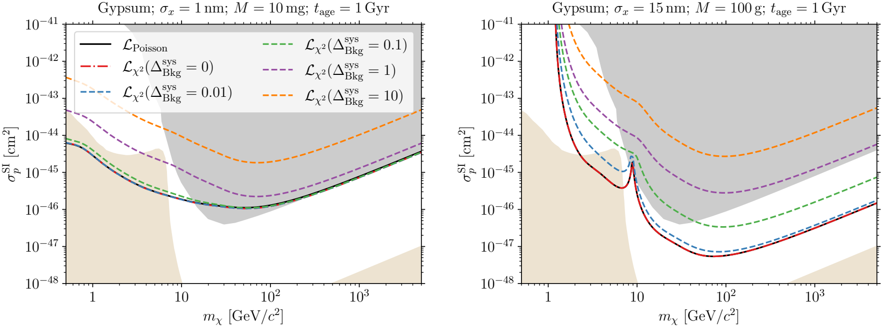

Sensitivity for different ^{238}U concentrations

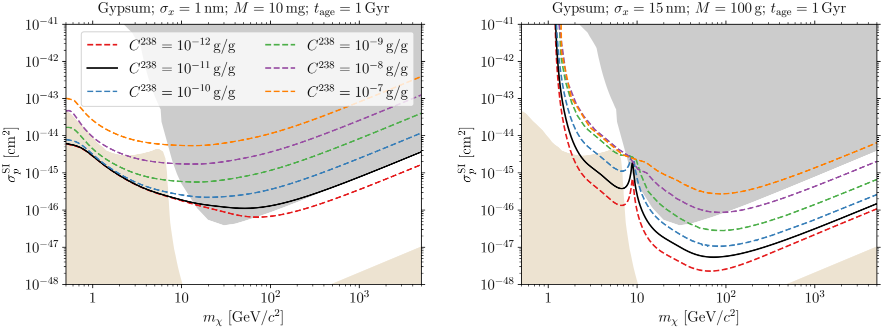

Mineral detectors can probe ultra-heavy dark matter

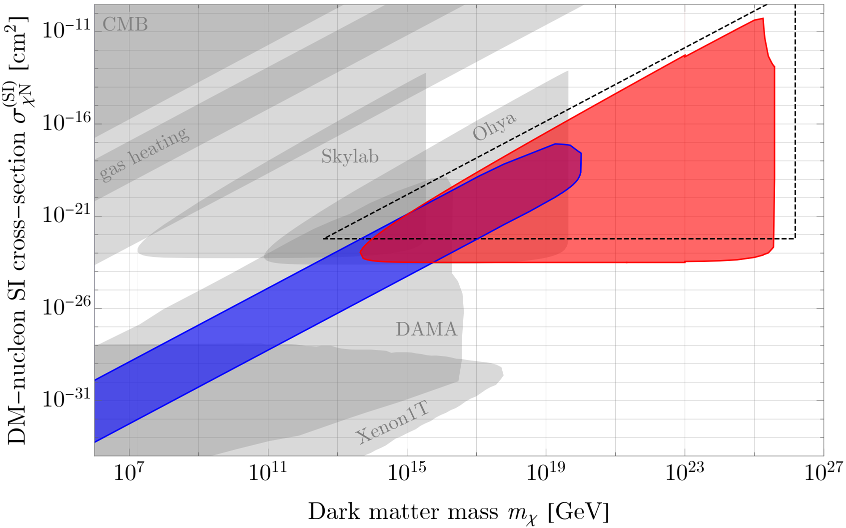

Figure: 2105.06473

Multiple nuclei and large ϵ allow for optimal $\Delta m_X / m_X$

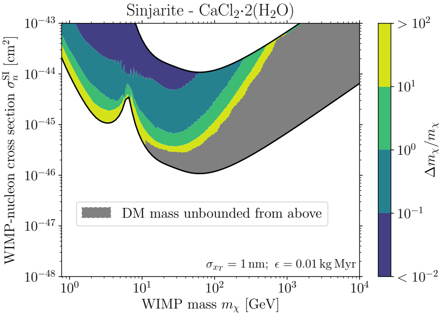

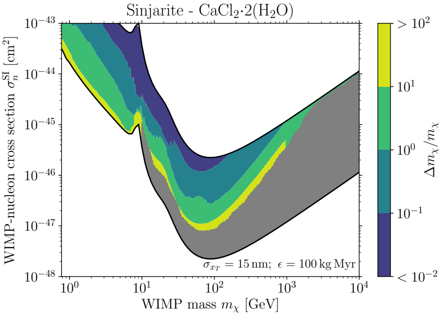

Mineral detectors can look for signals “averaged” over geological timescales or for time-varying signals

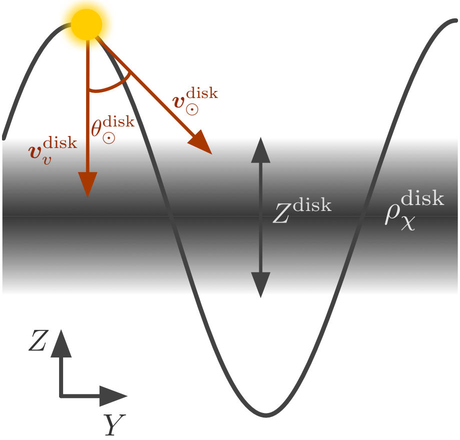

Figure: Dark Disk cartoon, 2107.02812

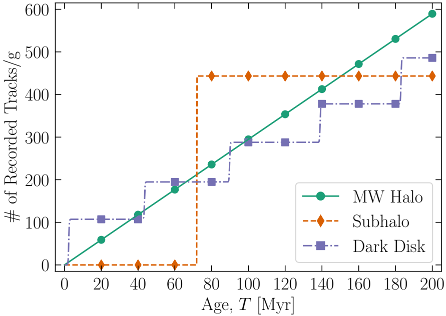

Figure: Time dependent DM signals in series of gypsum detectors for $m_X^{\rm disk} = 100\,\mathrm{GeV}$, $\sigma_{Xp}^{\rm disk} = 10^{-43}\,\mathrm{cm}^2$ and $\Sigma^{\rm disk} = 10 M_\odot/\mathrm{pc}^2$, 2107.02812

Measure time-varying signals with a series of samples

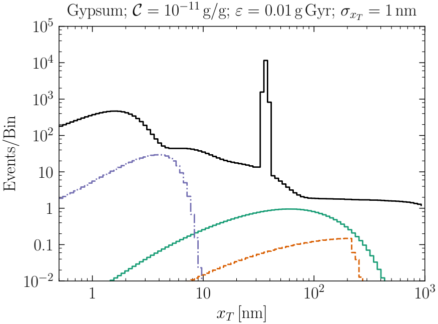

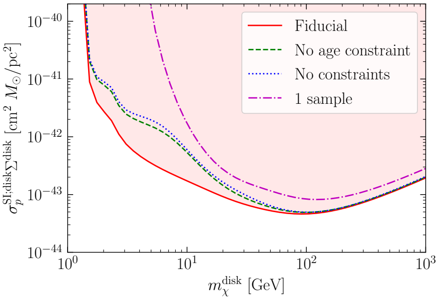

Dark disk transit every ~ 45 Myr

Spectra from dark disk crossing, MW halo, **combined backgrounds**

$m_X^{\mathrm{disk}} = 100\,\mathrm{GeV}\ \sigma_{Xp}^{\mathrm{disk}} = 10^{-43}\,\mathrm{cm}^2$

$m_X = 500\,\mathrm{GeV}\ \sigma_{Xp} = 5 \times 10^{-46}\,\mathrm{cm}^2$

Ages $t = 20, 40, 60, 80, 100$ Myr

- Systematic uncertainty $\Delta_t = 5\%$, $\Delta_M = 0.1\%$, $\Delta_C = 10\%$, $\Delta_\Phi = 100\%$
- > 1 samples more important

Geomagnetic field deflects lower energy CR primaries

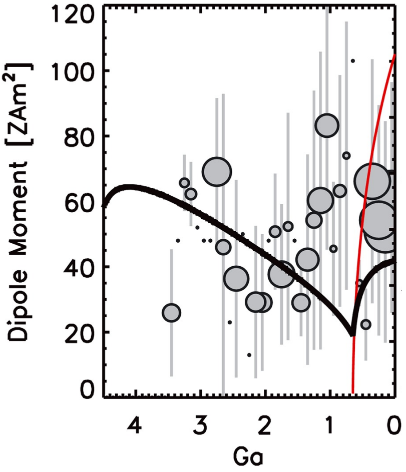

Figure: Driscoll, P. E. (2016), *Geophys. Res. Lett.*, 43, 5680-5687

Rigidity $p_{CR}/Z_{CR} \simeq E_{CR}$ for CR protons

- Rigidity cutoff $\propto M_{dip}$ truncates atmospheric ν spectrum at low E_ν
- Maximum cutoff today $\sim 50\,\mathrm{GV}$
- Recall CR primary $E_{CR} \gtrsim 10\,E_\nu$

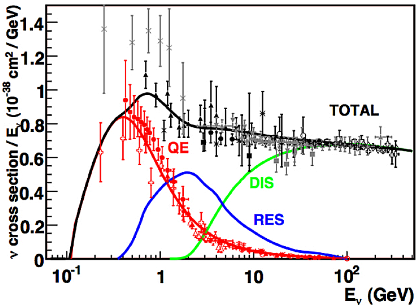

Recoil spectra from atmospheric ν's incident on NaCl(P)

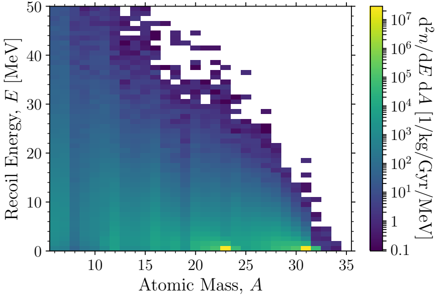

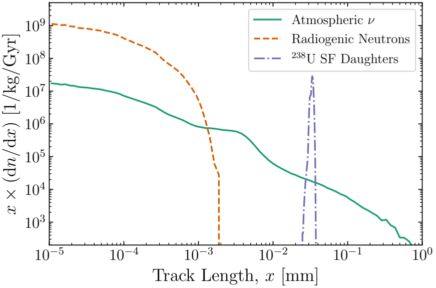

Recoils of many different nuclei

- Low energy peak from QE neutrons scattering ^{23}Na, ^{31}P
- High energy tail of lighter nuclei produced by DIS

Background free regions for $\gtrsim 1\,\mu$m

- Radiogenic n-bkg confined to low x, regardless of target
- Subdominant systematics from atmosphere, heliomagnetic field

Sensitivity to galactic CC SN rate depends on C^{238}

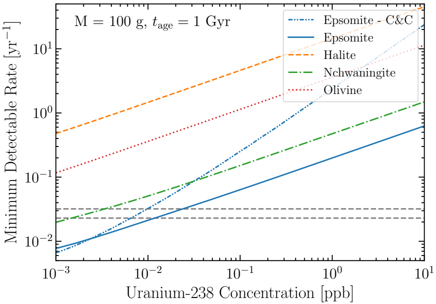

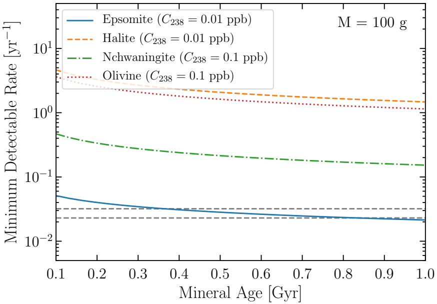

Epsomite [$\rm Mg(SO_4)\cdot 7(H_2O)$]
Halite [NaCl]

Nchwaningite [$\rm Mn_2^{2+}SiO_3(OH)_2\cdot(H_2O)$]
Olivine [$\rm Mg_{1.6}Fe_{0.4}^{2+}(SiO_4)$]

Difficult to pick out time evolution of galactic CC SN rate

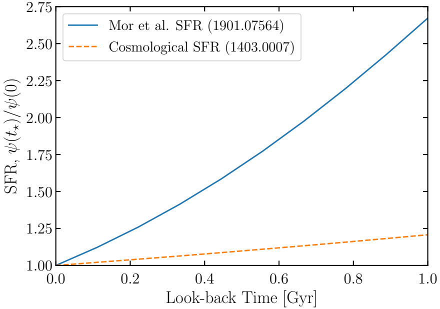

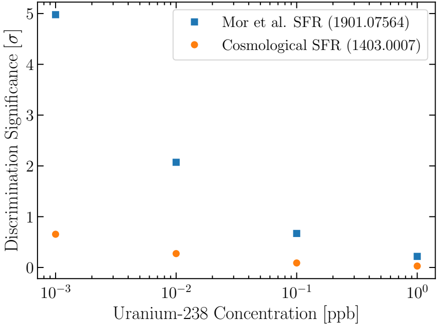

Coarse grained cumulative time bins

- 10 Epsomite paleo-detectors
- 100 g each, $\Delta t_{\rm age} \simeq 100\,{\rm Myr}$

Determine σ rejecting constant rate

Could only make discrimination at 3σ for $\mathcal{O}(1)$ increase in star formation rate with $C^{238} \lesssim 5\,{\rm ppt}$

Could use large exposure to differentiate between scenarios

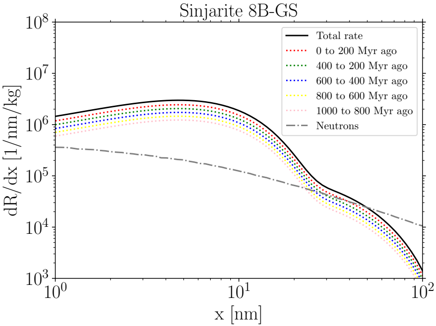

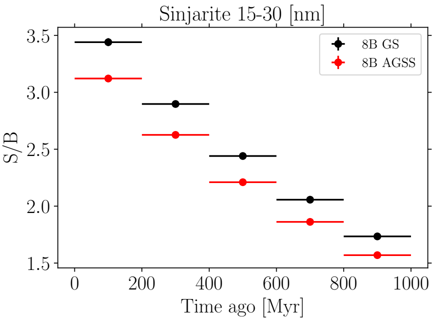

Could measure ^8B flux over time

- Higher $E_\nu \Rightarrow$ longer tracks
- Highly dependent on solar core temperature with flux $\propto T^{24}$
- Sensitive to metallicity model

100 g samples with 15 nm resolution

- Look in single bin $15 - 30\,\mathrm{nm}$
- Assume $\Delta_t \sim 10\%$, $\Delta_C = 10\%$
- $N_{\rm tot}^{\rm GS} \sim (1.63 \pm 0.05) \times 10^6$
  $N_{\rm tot}^{\rm AGSS} \sim (1.52 \pm 0.05) \times 10^6$